remote sensing

MDPI

Article

Identify Tea Plantations Using Multidimensional Features Based on Multisource Remote Sensing Data: A Case Study of the Northwest Mountainous Area of Hubei Province

Pengnan Xiao [1], Jianping Qian [1,*], Qiangyi Yu [1], Xintao Lin [1], Jie Xu [2] and Yujie Liu [3]

[1] State Key Laboratory of Efficient Utilization of Arable Land in China, Key Laboratory of Agricultural Remote Sensing (AGRIRS) Ministry of Agriculture and Rural Affairs, Institute of Agricultural Resources and Regional Planning, Chinese Academy of Agricultural Sciences, Beijing 100081, China; xiaopengnan@caas.cn (P.X.); yuqiangyi@caas.cn (Q.Y.); linxintao@caas.cn (X.L.)
[2] Faculty of Resources and Environmental Science, Hubei University, Wuhan 430062, China; 20220105@hubu.edu.cn
[3] College of Urban and Environmental Sciences, Central China Normal University, Wuhan 430079, China; liuyj@mails.ccnu.edu.cn
* Correspondence: qianjianping@caas.cn

Abstract: Accurate identification of tea plantation distribution is critical for optimizing agricultural practices, informing land-use policies, and preserving ecological balance. However, challenges persist in mountainous regions with persistent cloud cover and heterogeneous vegetation, where conventional methods relying on single-source remote sensing features face limitations due to spectral confusion and information redundancy. This study proposes a novel framework integrating multisource remote sensing data and feature optimization to address these challenges. Leveraging the Google Earth Engine (GEE) cloud platform, this study synthesized 108 spectral, textural, phenological, and topographic features from Sentinel-1 SAR and Sentinel-2 optical data. SVM-RFE (support vector machine recursive feature elimination) was employed to identify the optimal feature subset, prioritizing spectral indices, radar texture metrics, and terrain parameters. Comparative analysis of three classifiers, namely random forest (RF), support vector machine (SVM), and decision tree (DT), revealed that RF achieved the highest accuracy, with an overall accuracy (OA) of 95.03%, a kappa coefficient of 0.95. The resultant 10 m resolution spatial distribution map of tea plantations in Shiyan City (2023) demonstrates robust performance in distinguishing plantations from forests and farmlands, particularly in cloud-prone mountainous terrain. This methodology not only mitigates dimensionality challenges through feature optimization but also provides a scalable solution for large-scale agricultural monitoring, offering critical insights for sustainable land management and policy formulation in subtropical mountainous regions.

Keywords: Google Earth Engine; tea plantation; Sentinel-1; Sentinel-2; feature selection

check for updates

Academic Editor: Guido D'Urso

Received: 18 November 2024
Revised: 16 February 2025
Accepted: 28 February 2025
Published: 4 March 2025

Citation: Xiao, P.; Qian, J.; Yu, Q.; Lin, X.; Xu, J.; Liu, Y. Identify Tea Plantations Using Multidimensional Features Based on Multisource Remote Sensing Data: A Case Study of the Northwest Mountainous Area of Hubei Province. *Remote Sens.* **2025**, *17*, 908. https://doi.org/10.3390/rs17050908

Copyright: © 2025 by the authors. Licensee MDPI, Basel, Switzerland. This article is an open access article distributed under the terms and conditions of the Creative Commons Attribution (CC BY) license (https://creativecommons.org/licenses/by/4.0/).

1. Introduction

Tea is one of the three most popular drinks in the world (together with coffee and cocoa) and an essential cash crop for global agriculture, particularly in many developing nations. The tea tree (Camellia sinensis) is an evergreen broad-leaved perennial shrub that is commonly grown in tropical and subtropical mountains [1,2]. China is the world's foremost producer of tea, with a cultivation area of 3307.8 thousand hectares and a production volume of 3.164 million tons as of 2021. The fast spread of tea plantations has resulted in an

increase in tea production, which has subsequently facilitated local economic development. However, this expansion has also had a series of negative consequences, including a reduction in forest resources, biodiversity, and ecosystem services [3]. Consequently, precise identification of the distribution range of tea plantations holds scientific importance for relevant authorities in formulating suitable land policies, optimizing tea plantation practices, mitigating tea plantation diseases, estimating tea production, and safeguarding the ecological environment.

The conventional monitoring approach for tea plantations mostly relies on statistical reporting and field measurements, which are inefficient, inaccurate, costly, and incapable of providing continuous oversight [4]. Remote sensing, known for its real-time identification and its convenience and efficiency, is frequently employed in yield estimation and crop monitoring [5], but its use in determining the geographical distribution of tea plantations remains limited due to the challenges posed by tea being a perennial evergreen plant often grown in cloud-covered areas and intercropped with other vegetation [6]. The accuracy of tea plantation identification is impacted by the rise in mixed pixels in medium- and low-resolution remote sensing images, which results from the spectral properties of tea plantations being easily confused with similar vegetation types such as orchards and young woods. Therefore, relying on a single feature, whether spectral [7,8], textural [9–11], or topographic, makes it difficult to achieve the desired accuracy in identifying tea plantations. The challenges of mixed spectral information and cloud interference in tea plantations can be effectively addressed by incorporating a variety of features, including spectral, topographic, and radar characteristics [3]. However, the inclusion of high-dimensional features can result in information redundancy between features, and the "curse of dimensionality" can be induced by the combination of all features, which can affect both classification efficiency and accuracy to varying degrees [4]. Improving the general accuracy of remote sensing detection in tea plantations necessitates addressing the issue of multisource feature integration and creating efficient feature selection methods.

The main remote sensing classification algorithms for tea plantations include support vector machine (SVM) [4], decision tree (DT) [12], random forest (RF) [13], object-oriented [14], neural network [15], and deep learning [16]. The advantage of object-oriented classification lies in constructing a set of pixels with the same spectral, texture, and spatial features, thereby representing the relationships between geographic entities. However, object-oriented analysis's classification success is mostly dependent on picture segmentation, and choosing the correct image segmentation parameters requires extensive experimentation and, to some extent, relies on human subjective experience, which is not conducive to practical applications and comparisons of results [17]. In recent years, with an increase in its widespread use, deep learning has gradually been utilized in the identification of tea plantations. However, deep learning algorithms require complex hardware and software configurations, which are beyond the means, in terms of time and capability, for some large-scale, high-spatial-resolution tea plantation extraction research [18]. Relatively speaking, algorithms such as pixel-based DTs, SVMs, and RFs can analyze high-dimensional massive feature variables without requiring complex parameters or high computational environments. They are easy to operate and implement and have good classification performance [19,20]. Due to the different performance and characteristics of the three types of classifiers mentioned above, there is currently insufficient exploration of whether the responses of different classifiers to different feature types are consistent. Therefore, it is of great research value to assess and contrast, using particular remote sensing image data, the performance of the three classifier types mentioned above in tea plantation remote sensing recognition.

The optimization of remote sensing features and identification of tea plantations at a large regional scale places high demands on data and computational volume. The previous single-machine classification with slow classification speed and low efficiency is no longer able to meet the requirements for large-scale extraction of land features. In the context of the big data era, the Google Earth Engine (GEE) cloud platform, leveraging Google's powerful computing capabilities and massive online data, has changed the traditional data processing workflow of remote sensing software, providing possibilities for processing and analyzing vast amounts of data from remote sensing [21]. Users can greatly reduce the workload of data acquisition and processing by using a huge amount of geographic data products published on the GEE platform, combined with their own needs, to achieve online computing operations. Therefore, building a multisource feature system for tea plantations based on the GEE cloud platform—combining feature selection algorithms and multiple classifiers to accurately extract tea plantation information—to achieve the goal of improving computational efficiency and reducing costs has great practical significance.

Due to the interference of cloudy and rainy weather and the heterogeneity of tea plantation landscapes, accurately mapping tea plantations in Shiyan City, Hubei Province, is challenging. This study proposes a tea plantation detection method based on feature optimization using Google Earth Engine and Sentinel-1 and Sentinel-2 data in order to overcome these problems. This study's primary goal is to address two questions: (1) How to obtain the optimal feature combination representing the tea plantation from the large number of features obtained? (2) How to compare multiple classification methods to determine the most accurate one? The core innovation of this study lies in optimizing feature selection from multi-dimensional remote sensing data to achieve precise tea plantation identification, while simultaneously maintaining the overall classification performance. This study is structured as follows: First, Section 1 introduces the background and objectives. Next, Section 2 describes the study area and data. Subsequently, Section 3 details the methodology, including feature extraction, optimization, and classification. Following this, Section 4 presents the results, focusing on feature selection, accuracy comparison, and spatial distribution. Then, Section 5 discusses the findings and limitations. Finally, Section 6 concludes with key contributions and implications for sustainable tea plantation monitoring.

2. Materials

2.1. Research Area

Shiyan is located in Northwestern Hubei Province, in the hinterland of Qinba Mountainous region and the middle and upper reaches of the Han River, straddling latitude 31°30′~33°16′ north and longitude 109°29′~111°16′ east. Shiyan is almost 200 km long from east to west and 195.5 km from north to south. Shiyan has eight county-level administrative districts with an overall area of 23,680 square kilometers, including three municipal districts, one county-level city, and four counties (Figure 1). Shiyan is located in the mid-latitude region with a subtropical monsoon climate. The domain experiences an average annual temperature of 15.4 °C, an extreme maximum temperature of 41.9 °C, and an extreme minimum temperature of minus 11.9 °C. Shiyan receives the highest rainfall in the four months of June, July, August, and September and an average of 769.6 mm each year, with precipitation amounting to 456 mm, accounting for 59.2% of the annual rainfall. There is slightly more rainfall in the southeast than in the northwest.

One of Hubei Province's four primary tea-producing regions is Shiyan City, and its topography, climate, and light conditions are suitable for tea growth. The tea industry has become a pillar industry for farmers in the mountainous areas of the city to increase their income and attain wealth and a model industry to lead the development of modern agriculture in the mountainous areas. Tea trees are evergreen plants that are widely planted

in Shiyan City's flat and hilly regions (Figure 1), and the region's tea plantations are often dispersed and modest. Tea plantations have distinct planting traits and management techniques in contrast to other crops, evergreen forests, and plantations. Every year, tea trees start to sprout in March, and the harvest season lasts from March to October. April and October are the primary picking seasons for spring and fall tea, respectively.

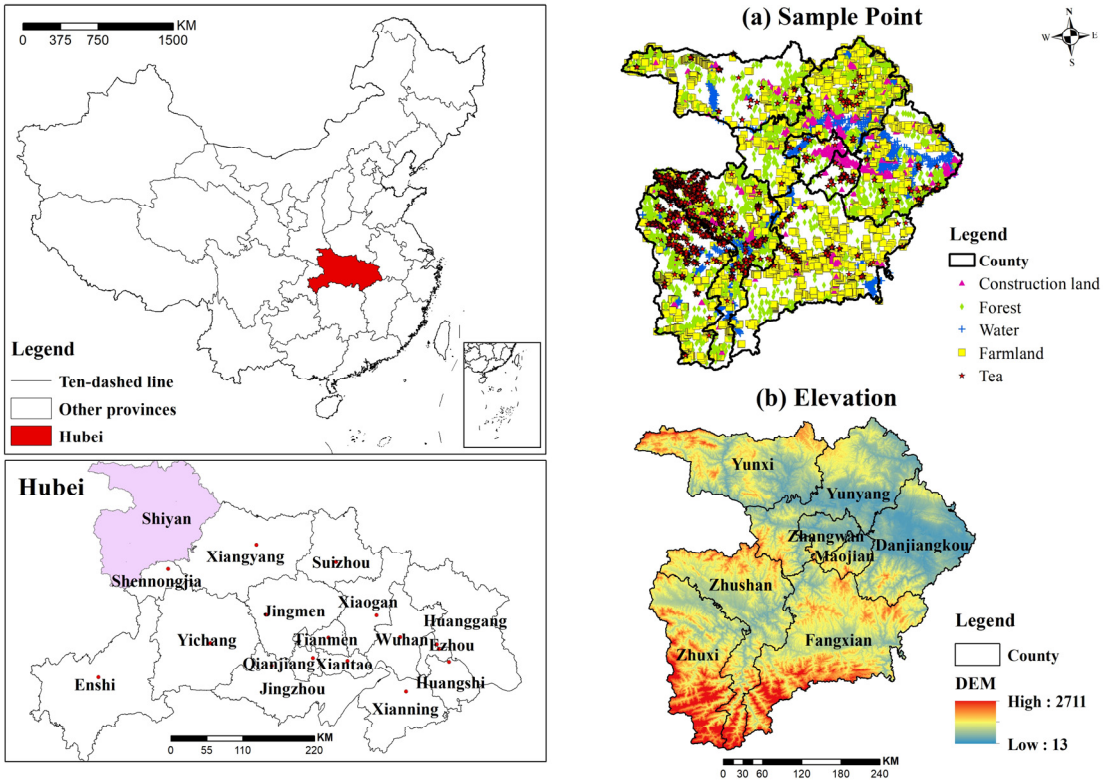


Figure 1. Study area layout.

2.2. Data Source

2.2.1. Sample Selection

In this study, based on the actual distribution of land types, the study area's land cover types were divided into five categories: construction land, farmland, forest, tea plantation, and water. According to the acquisition time of S1 and S2 image data, the acquired sample points were visually interpreted point by point in the corresponding Google Earth images, and a total of 11,958 sample point data were collected in Shiyan City in 2023, including 1507 construction land, 3486 farmland, 3548 forest, 2246 tea plantation, and 1168 water. To ensure the accuracy and representativeness of the sample data, the selection process considered land cover types, terrain characteristics (e.g., slope, aspect, and altitude), and the spatial heterogeneity of tea plantations. Specifically, tea plantation sample points encompassed different planting densities (e.g., densely and sparsely planted tea plantations). Additionally, to improve the classification model's performance in complex landscapes, a subset of sample points was deliberately chosen from land types that are challenging to distinguish from tea plantations, such as orange orchards. Specific types of sample data and distribution are shown in Figure 1a.

Tea plantations and orange orchards, while sharing similar texture features in Google Earth images, show distinct temporal signatures in both optical and radar data, helping to distinguish these two perennial crops (Figure 2a,b). Farmland presents clear seasonal patterns in both optical and radar data, with two distinct peaks in NDVI indicating double-cropping practices, while the SAR backscatter varies with crop growth stages and field

conditions (Figure 2c). As seen in Figure 2d, construction land exhibits unique characteristics in both optical and SAR data. For optical indices, pixels with an LSWI value of less than 0 for over 90% of observations in a given year are typical of construction land [22]. The SAR backscatter (VV and VH) shows relatively high and stable values throughout the year due to double bounce scattering from buildings. Forest demonstrates distinctive temporal patterns, with over 90% of LSWI observations greater than 0 and the minimum EVI greater than 0 throughout the year (Figure 2e). The SAR backscatter shows moderate values with slight seasonal variations due to changes in vegetation density and moisture content. As seen in Figure 2f, The characteristic of water pixels shows distinct patterns in both optical and radar data. For optical indices, mNDWI is higher than the EVI or NDVI, and more than 75% of the observed values in a year have an EVI of less than 0.1 [23]. In terms of radar backscatter, water bodies show characteristically low VV and VH values (around −20 dB) due to specular reflection.

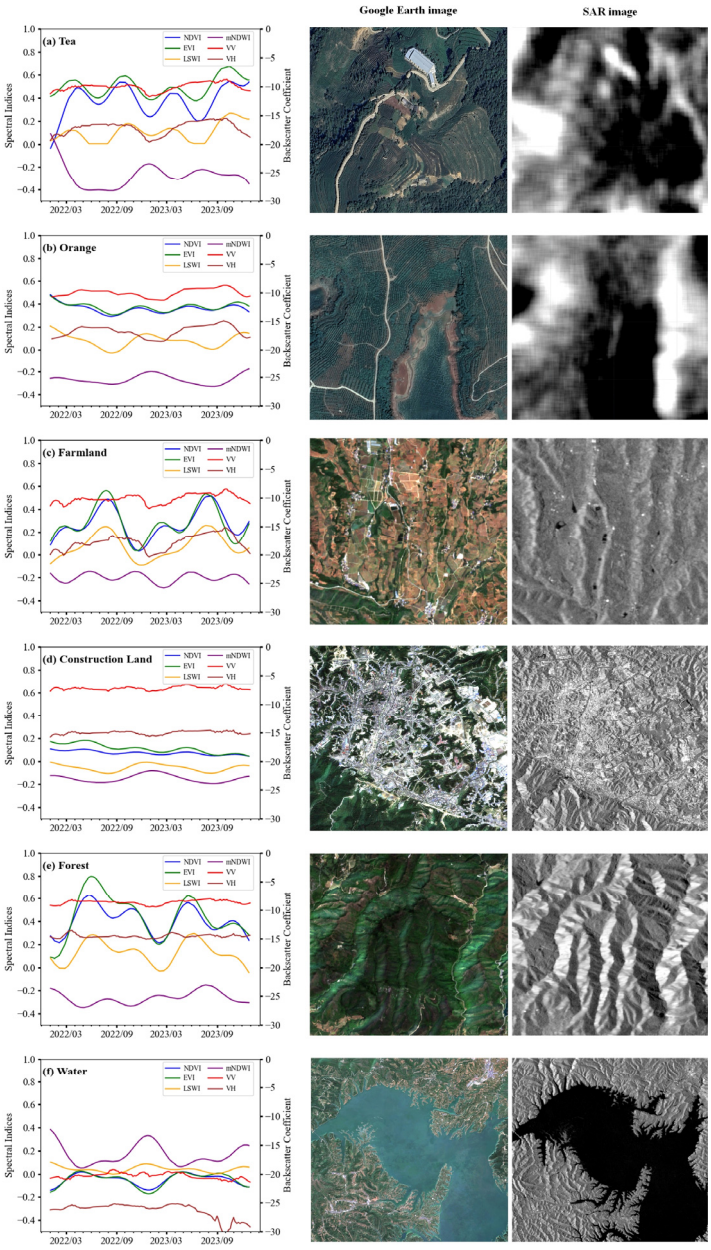


Figure 2. Time series of vegetation indices for typical land cover.

2.2.2. Remote Sensing Data

All remote sensing data are drawn from and processed through the GEE cloud platform, including Sentinel-1 (S1) radar data and Sentinel-2 (S2) multispectral data (Table 1). High temporal and geographic resolution are possessed by Sentinel-1 and Sentinel-2, which provide high-quality data for remote sensing interpretation. The data used for S2 are radiometrically calibrated and geometrically corrected Level-1C products, which contain 13 spectral bands and 3 QA bands, with cloud mask information found in the QA60 band. For the S2 images, CLOUDY_PIXEL_PERCENTAGE is used to filter the images with cloud pixel percentage less than 20%, the values of Bit10 and Bit11 of QA60 are set to be less than 0 to remove cirrus and thick clouds, and month-by-month synthesis is performed. The specific process is referred to in the literature [3,24]. Additionally, this study created a map of the coverage of remote sensing images and evaluated the quantity and quality of the data (Figure A1). The Sentinel-1 data used in this study consists of Ground Range Detected (GRD) scenes from C-band Synthetic Aperture Radar (SAR) instrument operating at 5.405 GHz. The collection includes dual-polarization (VV and VH) backscatter coefficients at 10 m resolution.

Table 1. Summary of datasets.

Dataset	Access Platform/Link	Time Range	Spatial Resolution	Purpose
Sentinel-1 SAR (GRD)	Google Earth Engine https://developers.google.com/earth-engine/datasets/catalog/COPERNICUS_S1_GRD (accessed on 30 September 2024)	2023	10 m	Radar backscatter analysis; texture feature extraction in cloudy regions
Sentinel-2 MSI (Level-1C)	Google Earth Engine https://developers.google.com/earth-engine/datasets/catalog/COPERNICUS_S2_HARMONIZED (accessed on 30 September 2024)	2023	10 m (optical bands)	Spectral and vegetation index calculation; phenological feature extraction
SRTMGL1_003 DEM	Google Earth Engine https://developers.google.com/earth-engine/datasets/catalog/USGS_SRTMGL1_003 (accessed on accessed on 30 September 2024)	2000	30 m (resampled to 10 m)	Terrain parameter derivation (elevation, slope, aspect)
Google Earth Imagery	Google Earth Pro	2023	Sub-meter (~0.5 m)	Sample point collection and visual validation of land cover types
Field Survey Samples	Field campaigns in Shiyan City	2023	/	Training and validation data for classification accuracy assessment

2.2.3. Topographic Data

The nearly global-scale digital elevation model (DEM) SRTMGL1_003 product from the Shuttle Radar Topography Mission (SRTM) is utilized, with a spatial resolution of 30 m. On the GEE platform, the resample and reproject functions are applied to adjust the resolution to 10 m, and the data are cropped according to the administrative boundary of Shiyan City.

3. Methods

The GEE cloud platform was used to rapidly acquire and process S1 and S2 data, as well as topographic data that covered Shiyan City. On this basis, spectral features, texture features, and topographic features were extracted. In order to achieve the most optimal extraction scheme for tea plantations and ultimately obtain the thematic spatial distribution map of tea plantations in Shiyan City in 2023, the recursive elimination algorithm was implemented. Six experimental groups were established in accordance with the selected

feature variables, and RF, DT, and SVM classifiers were employed for classification. Figure 3 illustrates the technical flow chart in its entirety.

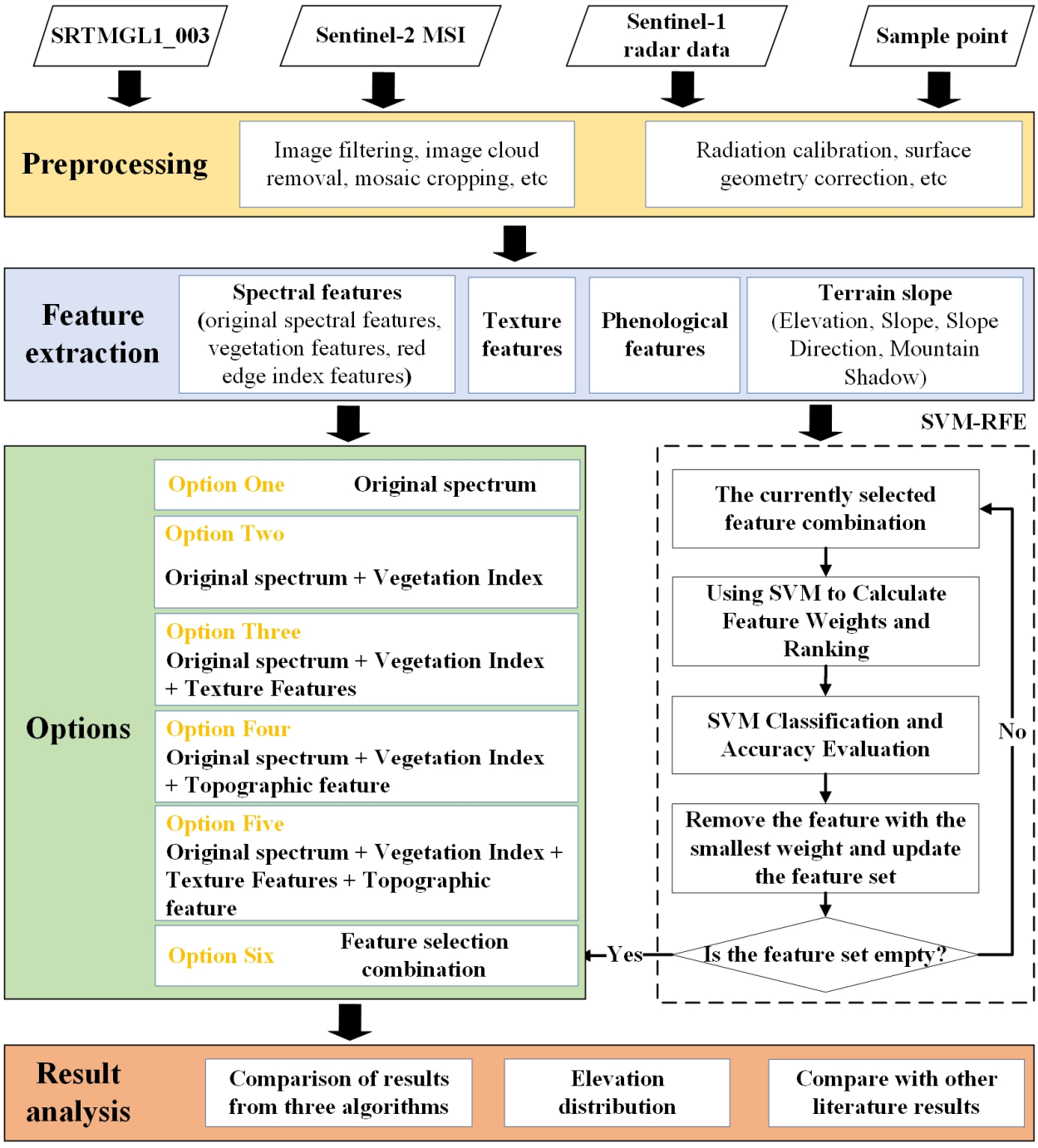


Figure 3. Technical workflow of tea plantation identification.

3.1. Feature Extraction

(1) Spectral characterization. Based on the preprocessed image ensemble, the original six bands and 10 vegetation indices were used (shown in Table 2), including EVI [25], NDWI [26], NDVI [27], NDTI [28], GCVI [29], SAVI [30], gNDVI [31], mNDWI [32], LSWI [33], and mNDVI [32].

Table 2. Vegetation indices.

Index	Formula	No.
EVI	$2.5 \times (NIR - R)/(NIR + 6 \times R - 7.5 \times B + 1)$	(1)
NDWI	$(NIR - SWIR1)/(NIR + SWIR1)$	(2)
NDVI	$(NIR - R)/(NIR + R)$	(3)
NDTI	$(R - G)/(R + G)$	(4)
GCVI	$NIR/G - 1$	(5)
SAVI	$(NIR - R) \times (1 + L)/(NIR + R + L)$	(6)
gNDVI	$(NIR - G)/(NIR + G)$	(7)
mNDWI	$(G - SWIR1)/(G + SWIR1)$	(8)
LSWI	$(NIR - SWIR2)/(NIR + SWIR2)$	(9)
mNDVI	$(NIR - R)/(NIR + R + 0.16)$	(10)

Notes: NIR = near-infrared band. R = red band. G = green band. B = blue band. SWIR1 = short-wave infrared band. SWIR2 = short-wave infrared band. L = soil adjustment factor.

(2) Texture features. The principle of gray-level covariance matrix (GLCM) proposed by Haralick [10,34] is simple, easy to implement, highly adaptable, and robust, making it widely applicable in remote sensing image texture extraction [35]. Based on the texture information of radar images, their combination with optical data can improve classification accuracy for vegetation [4]. Therefore, utilizing the glcmTexture function in Google Earth Engine (GEE), this study computes the texture features of RGB_Gray [36], VV, and VH bands (Table 3) by applying a 4×4 window size, quantizing image intensities into 256 discrete gray levels, and employing a 3×3 spatial kernel with offset pairs $(-1, -1)$, $(0, -1)$, $(1, -1)$ and $(-1, 0)$. Additionally, the averaging parameter is enabled to generate rotation-invariant texture representations, with these parameter choices balancing computational efficiency and thorough texture analysis.

Table 3. Texture characteristics.

Feature	Description	Feature	Description
asm	Angular second moment	var	Variance
corr	Correlation	savg	Sum average
maxcorr	Maximum correlation	sent	Sum entropy
idm	Inverse difference moment	davr	Difference variance
savr	Sum of squares: variance	imcorr1	Information measure of correlation 1
ent	Entropy	imcorr2	Information measure of correlation 2
dent	Difference entropy	inertia	Inertia
diss	Dissimilarity	shade	Cluster shade
contrast	Contrast	prom	Cluster prominence

(3) Phenological characteristics. Phenology is the phenomenon of seasonal changes in the development or life cycle of animals and plants, such as plant germination, flowering, leaf shedding, animal migration, and reproduction [37,38]. The plant growth rhythm reflected by vegetation index time series data is utilized for identifying plant phenological periods [39]. This study extracted phenology using NDVI and methods [40], as shown in Figure 4. SOS (start of season) occurs at the beginning of March, representing the beginning of the growing season. EOS (end of season) is mid-November, representing the end of the growing season.

(4) Terrain features. Given that tea tree cultivation necessitates specific terrain conditions, the GEE platform was utilized to access SRTMGL1_003 data online to compute four prevalent terrain attributes: slope, aspect, elevation, and hillshade. These attributes were employed as four distinct bands in the feature construction process.

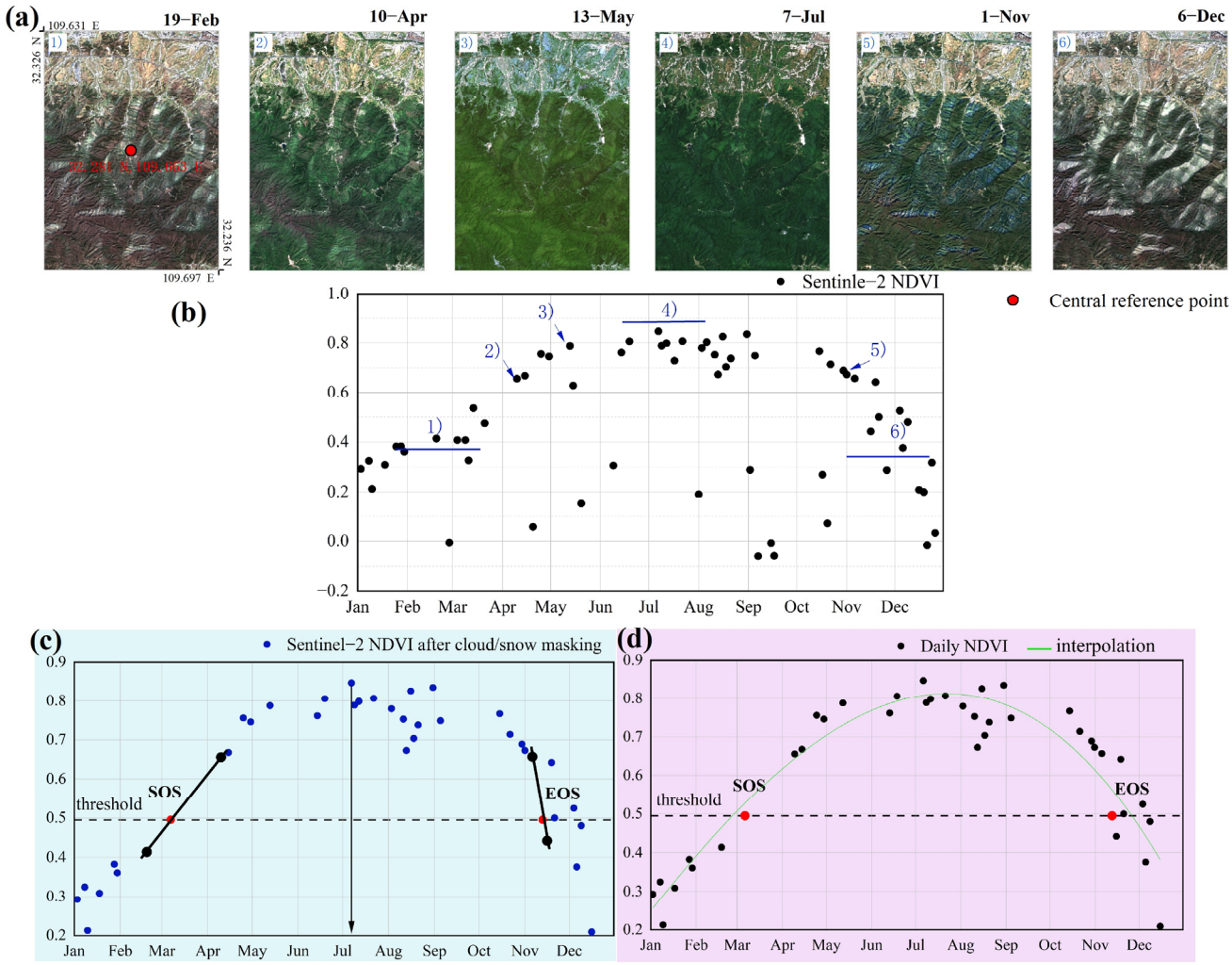


Figure 4. An example of the dynamics of vegetation for a selected tea plantation in Shiyan. (**a**) Sentinel-2 time series data in 2023 visualized as true color composites; (**b**) NDVI time series for 2023 corresponding to the true color composite in (**a**); (**c**) NDVI time series following cloud masking and snow filtering, where start of season (SoS) and end of season (EoS) correspond to the earliest and latest linearly interpolated NDVI values, respectively, above a threshold dynamically defined as 50% of the annual amplitude; and (**d**) application of the threshold method over a smoothed and interpolated time series.

(5) Feature optimization. In this study, the recursive elimination SVM algorithm is utilized for feature selection. Recursive feature elimination (RFE) is an integrated method that combines the SVM classification algorithm and RFE to achieve better results [4]. The specific flow of the SVM_RFE feature selection algorithm is shown in Figure 3. Firstly, all the features are utilized as the initial feature, SVM is used to calculate the feature weights, sort the features according to the size of the weights, remove the feature with the smallest feature weight each time, classify the features using SVM, and use both the total accuracy and the accuracy measured by the kappa coefficient evaluation criterion iteratively until the feature set is empty. Then, SVM outputs the combination of features with the highest accuracy evaluation.

A total of 108 features were computed in the GEE platform (Table 4). To determine the optimal scheme for tea plantation extraction, four experimental schemes were devised with two primary objectives: firstly, to identify the most effective approach for tea plantation extraction by comparing six experimental schemes (Table 5), and secondly, to identify the most significant feature variables by a feature selection technique, thereby achieving

dimensionality reduction of high-dimensional data and selecting the paramount feature variables for tea plantation extraction.

Table 4. Summary of features.

Features	Detail	Number
Original spectrum	Green, blue, red, Nir, Swir1, Swir2	6
Vegetation index	EVI, NDWI, NDVI, NDTI, GCVI, SAVI, gNDVI, mNDWI, LSWI, mNDVI	10
Harmonic characteristics	Phase, amplitude, value of each vegetation index	30
Texture features	18 texture features of RGB_Gray	18
	VV and VH and 18 texture features	38
Phenological characteristics	SOS, EOS	2
Topographic feature	Elevation, slope, aspect, hillshade	4
	Total	108

Table 5. Combination scheme.

No.	Feature Combination
1	Original spectrum
2	Original spectrum + vegetation Index
3	Original spectrum + vegetation index + texture features
4	Original spectrum + vegetation index + topographic feature
5	Original spectrum + vegetation index + texture features + topographic feature
6	Feature selection

3.2. Classification Methods

DT is a supervised classification technique that is based on data mining and knowledge discovery. It can be combined with various image data to create classification rules that are simple to comprehend and apply. It has been widely used in image classification and remote sensing information extraction [41]. The RF algorithm is a DT-based integrated learning technique that combines numerous integrated regression or classification trees. The algorithm generates a huge number of DTs using the bagging method, and the majority vote of all DTs determines the final classification result [42]. The RF method, which is widely used in various domains, including forestry and crop classification, has the advantages of quick training speed and not being easily overfitted when compared to other classification algorithms [43,44]. The basic idea behind the SVM algorithm [45], a nonparametric statistical learning technique, is to use preselected nonlinear relations to map the input vectors onto a high-dimensional feature space. Then, it finds the best classification hyperplane in this space to maximize the classification interval between two classes. SVMs have been widely employed in remote sensing research because of their great generalization capacity and the limited sample size that they require; these properties allow them to support classification in a high-dimensional feature space and achieve high accuracy in this space [46].

3.3. Accuracy Evaluation

In this study, thirty percent of the sample points are used for accuracy assessment, while seventy percent are used for training (Table 6). The classification performance of specific varieties is described by user accuracy (UA) and producer accuracy (PA), while the overall accuracy of tea plantation recognition is assessed using overall accuracy (OA) and kappa coefficients calculated from the confusion matrix.

Table 6. Accuracy verification.

Indicator	Calculation Formula
Overall accuracy (OA)	$OA = \frac{\sum_{k=1}^{n} x_{kk}}{\sum_{i,k=1}^{n} x_{ik}}$
Producer's accuracy (PA)	$PA(\text{class}_i) = \frac{x_{ii}}{\sum_{k=1}^{n} x_{ki}}$
User's accuracy (UA)	$UA(\text{class}_i) = \frac{x_{ii}}{\sum_{k=1}^{n} x_{ik}}$
F1-score	$\text{F1} - \text{score} = 2 \times \frac{UA \times PA}{UA + PA}$
Kappa coefficient	$\text{Kappa} = \frac{N\sum_{k=1}^{n} x_{ii} - \sum_{k=1}^{n} \left(\sum_{i=1}^{n} x_{ik} \hat{A} \cdot \sum_{i=1}^{n} x_{ki}\right)}{N^2 - \sum_{k=1}^{n} \left(\sum_{i=1}^{n} x_{ik} \hat{A} \cdot \sum_{i=1}^{n} x_{ki}\right)}$

Note: x_{kk} (number of correctly classified instances for class k); x_{ik} (number of instances classified as class k); x_{ki} (number of reference samples for class k); and x_{ii} (number of correctly classified instances for class i).

4. Results

4.1. Feature Selection

A total of 108 features were selected to participate in tea plantation extraction, and the results from the SVM_RFE algorithm can be seen in Figure 5, where the overall accuracy and the kappa coefficient are the mean values of ten-fold cross-validation. Figure 5a illustrates how, as the number of features increases from one to five, the total accuracy and kappa coefficient of the classification exhibit a rapidly growing trend, and the first five features are nir_mean, SAVI_mean, red_mean, VV_savg, and VH_savg. When the feature number is increased from 5 to 40, the overall accuracy and kappa coefficient of the classification grow steadily, and the features in decreasing order of importance are GCVI, NDVI_val, GCVI_val, RGB_gray_dent, RGB_gray_inertia, RGB_gray_diss, RGB_gray_shade, RGB_gray_prom, LSWI, blue, green, LSWI_val, mNDWI_val, SAVI_val, and mNDWI. After the number of features reaches 40, as the feature number increases, the classification accuracy tends to stabilize. As shown in Figure 5b,c, based on the statistical analysis of the spectral mean and variance of various land cover types using training sample points, it can be seen that the tea plantations in Shiyan City have a certain degree of separability with other land cover types in the red edge 1 band (B5), the near-infrared band (B8), shortwave infrared 1 band (B11), and shortwave infrared 2 band (B12) resulting in the selection of relevant vegetation indices based on the three bands in feature optimization. Therefore, this study selected the top 40 feature variables as the optimal feature variables to form the feature combination in Scheme 6, including six original spectral features, eight vegetation indices, twelve harmonic features, one phenological feature, twelve texture features, and one terrain feature.

The results of feature selection indicate that spectral properties, vegetation indices, and texture features play significant roles in the extraction of tea plantations, aligning with empirical observations. Shiyan City, situated in the mountainous region of Northwest Hubei Province, experiences year-round cloud and rain, and since radar images are unaffected by cloud cover and lighting, they are particularly useful for obtaining surface information in areas with severe cloud coverage and shadow effects. Furthermore, tea plantations are primarily located in hilly and mountainous regions with intricate landscapes, and their interiors are disorganized and disorderly, showcasing the interplay between tea trees, barren land, shrubs, artificial features, and other elements. Consequently, the average, entropy, and differences that are pertinent to the degree of texture regularity were chosen. Tea plantation planting has certain requirements for terrain, with a planting slope range of 5–25°. Therefore, the slope was selected in the feature optimization.

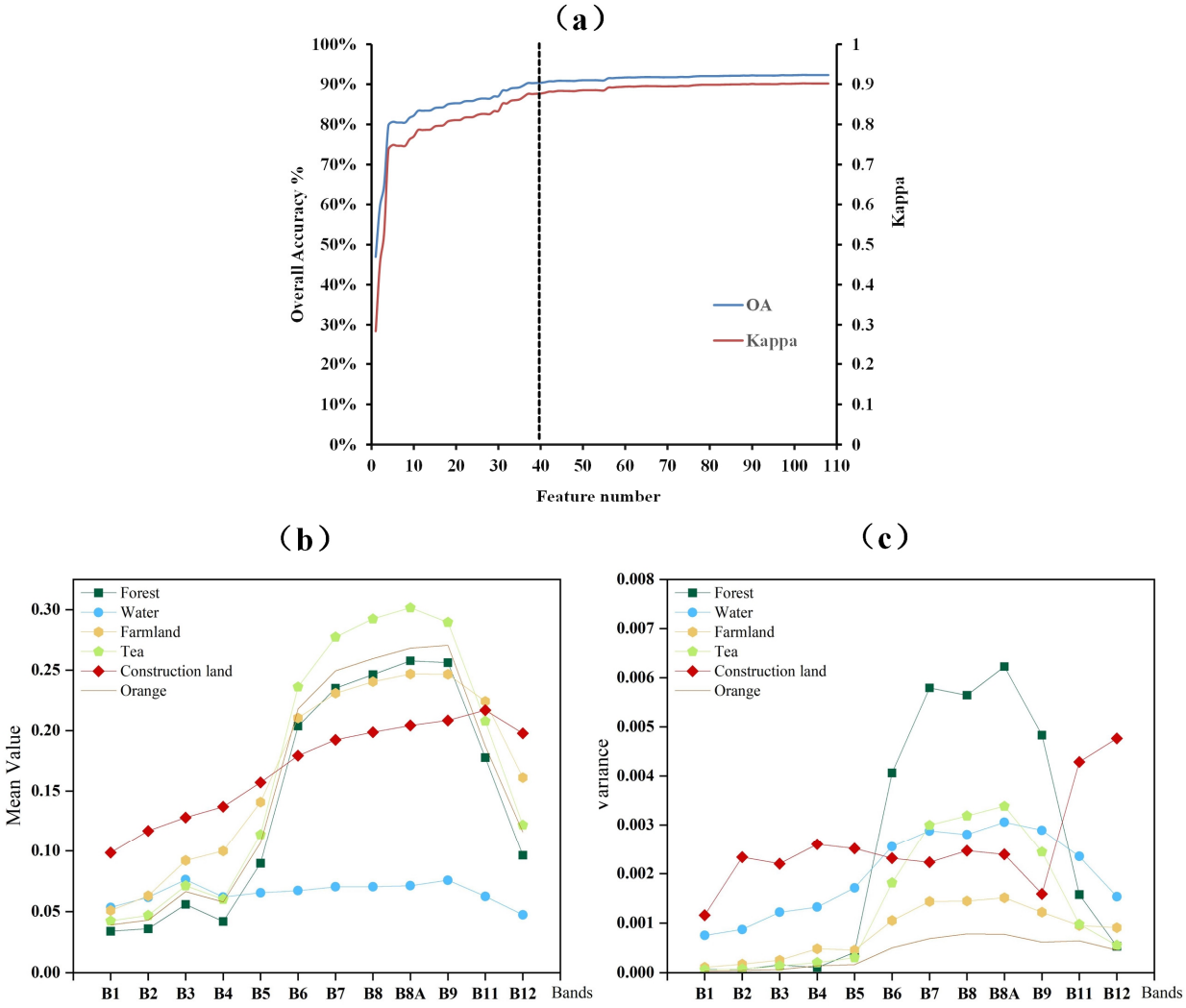


Figure 5. Feature selection results using SVM-RFE. (**a**) represents the results obtained with the SVM-RFE algorithm; (**b**) and (**c**) represent the mean values and variance of ground object spectral curves, respectively.

4.2. Comparison of Extraction Accuracy of Tea Plantations by Different Classification Methods

Based on feature optimization, the optimal classification features were obtained, and three commonly used supervised classification methods (SVM, DT, RF) were selected for tea plantation extraction and compared for accuracy. The results of classification obtained from various experimental schemes are distinct. Based on Table 7, it is clear that using the original spectral features alone for tea plantation extraction has an overall accuracy of 75%. This indicates that Sentinel-2 data's initial spectral properties offer some benefits for classifying land cover and further support the feature selection results. The overall accuracy of Scheme 2 was enhanced by 3.69% by the inclusion of vegetation indices in Scheme 1. Scheme 3 added texture features on the basis of Scheme 2, which improved the overall accuracy by 2.05%. The tea plantation's PA and UA both increased to over 84% with the inclusion of textural features. Furthermore, the inclusion of textural features further reduced the phenomenon of misclassification in tea plantations, and the UA of tea plantations increased by 1%. The addition of terrain features to Scheme 4 on the premise of Scheme 3 led to a 1.59% increase in overall accuracy. Scheme 5 enhanced the accuracy of Scheme 4 by incorporating texture and terrain features, culminating in a 0.62% overall improvement. After feature selection, with a kappa coefficient of 0.95 and an overall accuracy of 95.03%, Scheme 6 had the best extraction accuracy and was an improvement compared to Scheme

5. When the SVM-RFE feature selection technique is used, it successfully maintains the most significant land cover feature variables, reduces data dimensionality, maintains high accuracy, mitigates the influence of cross-redundant information on classification outcomes, shortens execution time, and enhances classification accuracy and efficiency.

Table 7. Classification accuracy statistics of different experimental schemes.

Experimental Schemes	OA/%			Kappa		
	SVM	RF	DT	SVM	RF	DT
1	75.70	86.56	80.00	0.68	0.87	0.80
2	81.92	90.25	82.72	0.77	0.90	0.83
3	88.50	92.30	84.16	0.85	0.92	0.84
4	86.45	93.89	86.98	0.83	0.94	0.87
5	90.79	94.51	87.90	0.88	0.95	0.88
6	90.42	95.03	88.59	0.88	0.95	0.89

Note: SVM, RF, and DT, respectively, represent support vector machine, random forest, and decision tree.

The confusion matrix is displayed in Table 8, with the highest overall accuracy in tea plantation extraction (Scheme 6). It is clear that forest land is the type that is most often mistaken for tea plantations. After texture and terrain features were added, the accuracy of tea plantation extraction was improved to some extent. Although there was still some confusion between tea plantations and forest land, the overall classification accuracy was 95.03%, and the kappa coefficient was 0.95. The highest user accuracy of tea plantations is 93.41%, and the producer accuracy is 88.65%.

Table 8. Confusion matrix with the highest overall accuracy.

Class	Forest	Water	Farmland	Tea	Construction Land	Orange	Total	UA/%
Forest	9669	0	76	160	1	2	9908	94.57
Water	0	3210	4	0	5	3	3222	99.72
Farmland	110	0	9385	148	69	6	9726	94.44
Tea	406	0	290	5546	1	13	6256	93.41
Construction land	17	1	58	3	4101	0	4193	95.61
Orange	20	0	54	79	0	694	847	96.65
PA/%	97.58	99.62	96.49	88.65	97.80	81.93		
OA/%: 95.03 Kappa: 0.95								

4.3. Spatial Distribution of Tea Plantations

4.3.1. Distribution of Tea Plantations in Shiyan

The GEE platform served as the foundation for this study, and SVM-RFE was used to select the optimal classification features from multiple sources, completing the distribution mapping of 10 m resolution tea plantations in Shiyan City in 2023. From a random selection of tea plantations to extract results for detailed display (Figure 6), it is clear that the tea plantation plot boundaries extracted based on our method are in good agreement with Google imagery and have high accuracy. The integration of Sentinel-1 SAR data provides valuable additional information about the texture and structure of tea plantations, as the backscatter characteristics in SAR imagery can help distinguish tea plantations from other vegetation types due to their unique planting patterns and canopy structure (Figure A2). From the spatial distribution map of tea plantations in Shiyan City, it is clear that the tea plantation areas in Shiyan City are mainly distributed in the southwest, central, and southern parts. On the county level, these areas can be divided into three levels: in the first level, Yunyang District, Yunxi County, and Danjiangkou City have a relatively lower

distribution of tea plantations; Zhangwan District, Maojian District, and Fangxian County constitute the second level; finally, the distribution of tea plantations is relatively higher in Zhushan County and Zhuxi County.

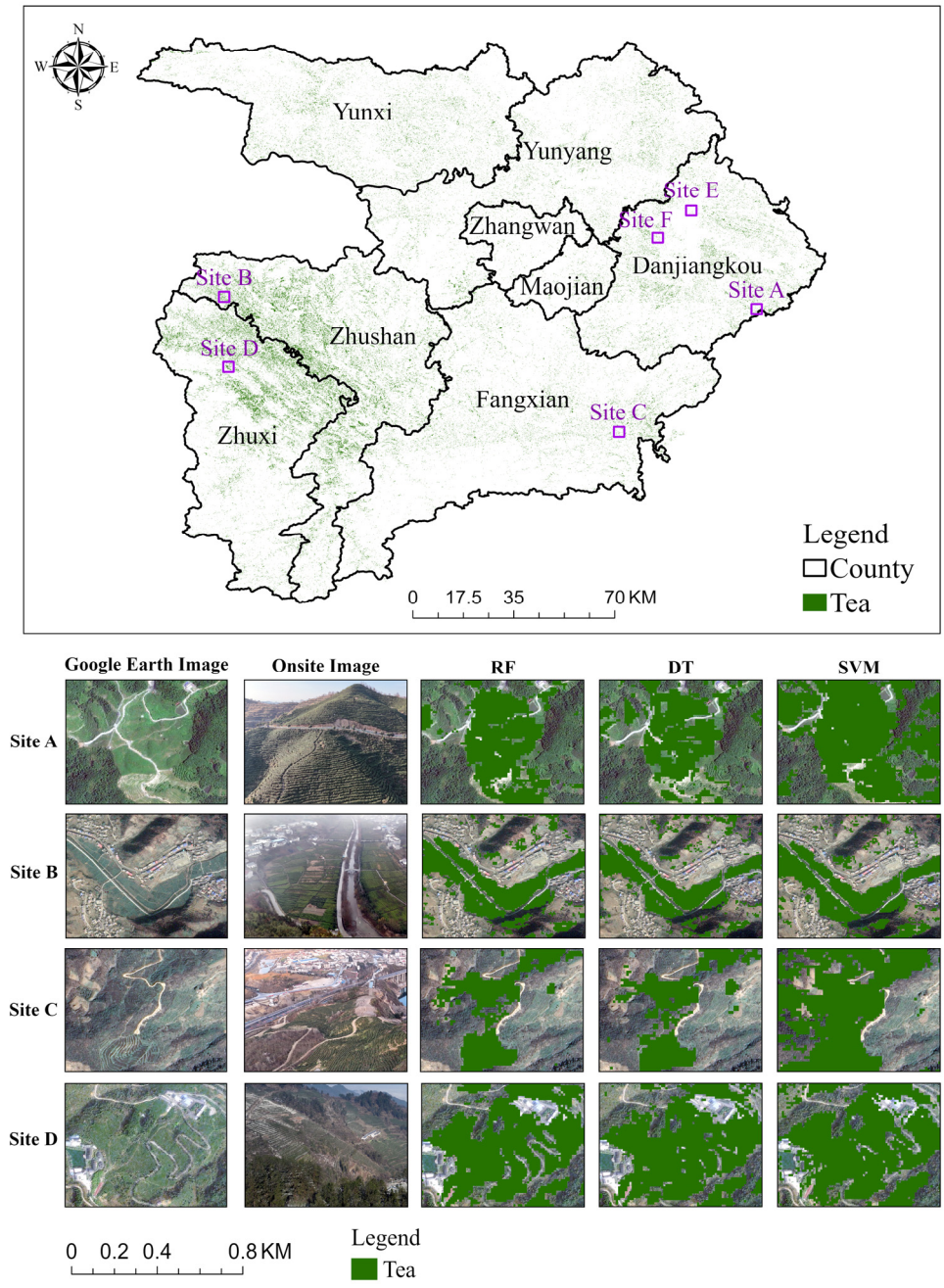


Figure 6. Spatial distribution of tea plantations in Shiyan City in 2023.

4.3.2. Elevation Distribution Characteristics of Tea Plantations

The further analysis results of the elevation and slope characteristics of tea plantations in Shiyan City are shown in Figure 7. This study established 11 height intervals at 100 m increments (Figure 7a). Tea gardens in Shiyan City exhibit a pattern of initially increasing and subsequently decreasing elevation. Tea plantations distributed within the elevation zone of 500–600 m account for the largest proportion among all intervals, with over 60% of tea plantations distributed within the range of 300–800 m. Taking 5° as one interval range, a total of 11 slope ranges were set (Figure 7b). The result shows that tea plantations in Shiyan City are mainly concentrated within the range of 5–25°, accounting for more than 50% of

the total area. Additionally, 90% of tea plantations are distributed in the gentle slope zone below 35°. These patterns are closely related to the environmental conditions required for tea plantation growth. Steep slopes, characterized by thin soil layers and poor water and nutrient retention, are unfavorable for the growth of tea trees.

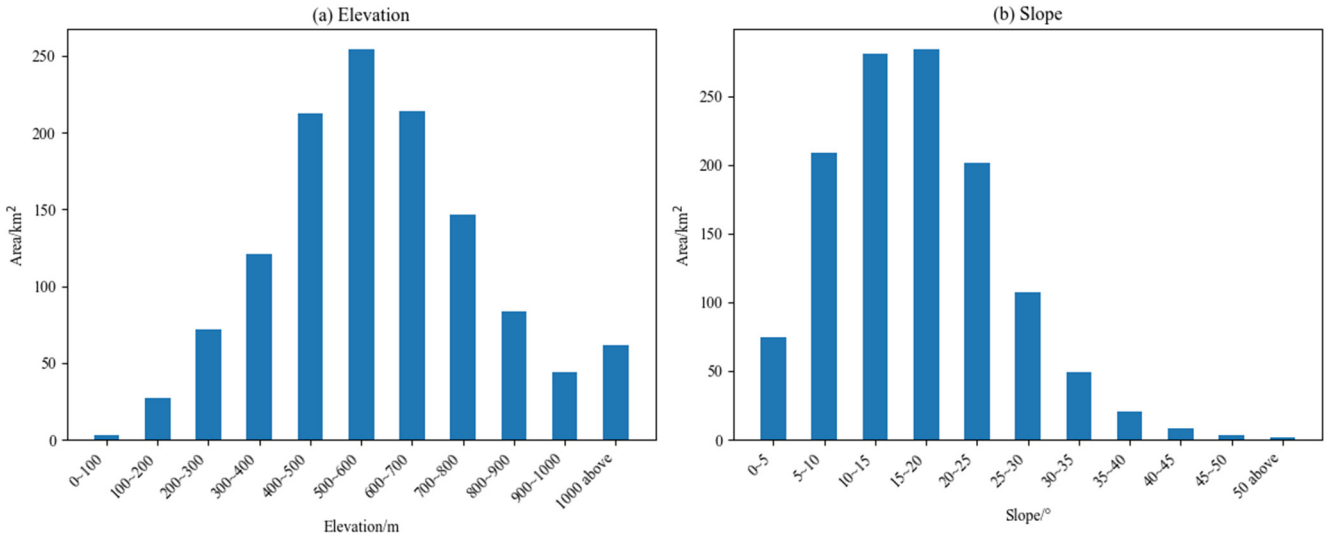


Figure 7. Area statistics of tea gardens in Shiyan City at different elevations and slopes in 2023.

5. Discussion

5.1. Comparison with Other Results

This study proposes a method suitable for large-scale tea plantation extraction research. In terms of feature selection, combining multisource features with appropriate feature selection algorithms, it was found that integrating multiple types of features can significantly improve classification accuracy. This mechanism not only fully utilizes the advantages of multisource information fusion but also effectively preserves the contribution of important features and reduces data dimensionality and correlation, thus achieving the effect of improving accuracy and computational efficiency. In terms of data processing, this study has utilized cloud computing technologies and greatly reduced the workload of data acquisition and preprocessing through the GEE cloud platform, providing a pathway for future provincial and even larger-scale thematic mapping. The advantage of this study lies in the completion of the 10 m resolution tea plantation information extraction work in Shiyan City using the GEE cloud platform, overcoming the problem of insufficient monitoring and computing capabilities for large-scale tea plantations. The extraction results can provide important decision-making assistance for the assessment of the ecological environment and for the growth and forecasting of Shiyan City's tea industry.

The errors in remote sensing of tea plantations in this study are mainly caused by the diversity in tea plantation scenery, which may result in more jumbled pixels and compromise the precision of tea plantation identification. Firstly, tea trees are often planted in rows, with a certain distance between each row, presenting a situation where tea trees are intertwined with bare soil in the image. Secondly, tea plantations are not only limited to tea trees but also have other features, such as bare soil, trees, and artificial objects, which present complex image features in the images, making it difficult to accurately extract tea plantation areas. Additionally, the study's findings show that the main objects of misclassification of tea plantations are forests and farmland. The main reason for this is that the spatial distribution of tea plantations and forests is similar, and some scattered tea plantations are distributed around or inside the forest, resulting in their misclassification as

forests. The similarity in spectral and texture features between tea plantations and farmland also leads to misclassification.

Peng et al. [47] used the MAP-Tea framework to achieve a map of Chinese tea plantations for the first time, making a significant contribution to tea plantation recognition. As shown in Figure 8, compared with their results, this study is more detailed in certain areas. In Site A and Site B, this study identified contiguous tea plantations in mountainous and flat areas. MAP-Tea divided a large area of citrus cultivation in the northwest of Shiyan City into tea plantations (Site E and Site F in Figure 6), and forest areas were divided into tea plantations.

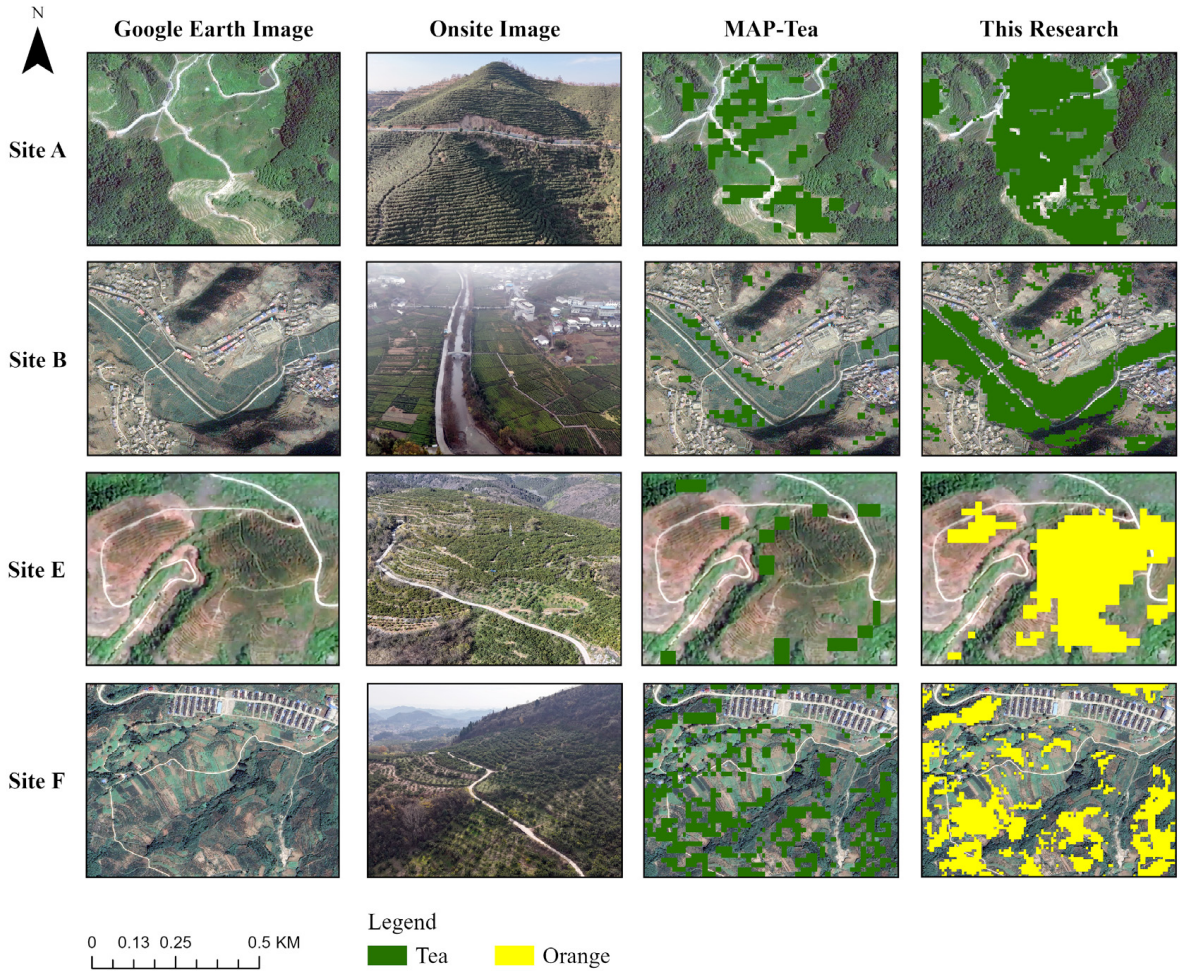


Figure 8. Comparison with MAP tea results.

5.2. Algorithmic Deficiencies of This Study

In summary, many scholars have achieved fruitful results in research based on different remote sensing data sources of spectral, texture, spatial, and area characteristics, using different classification algorithms to realize the extraction of tea plantations, disease and pest monitoring, yield prediction, etc. [48]. However, there are still some problems in the current research system that require further research and discussion.

From the viewpoint of data sources, optimizing the spatiotemporal resolution of remote sensing data and making efficient use of existing satellite resources are the basic problems faced by remote sensing identification of tea. Low-spatial-resolution data are affected by "mixed pixels"; these data are not suitable for remote sensing tea identification studies with finer spatial scales [49,50]. Medium- and high-resolution data are able to offer richer information on geometry, texture, structure, and contextual hierarchy and have

relatively higher classification accuracy and target recognition reliability; however, these data are problematic in terms of their lower data security rate [51,52]. Unmanned aerial vehicles (UAVs) and satellite remote sensing technologies have made it feasible to obtain image data with high spatial and temporal resolution. However, more thorough research is required in the fields of tea classification strategies and remote sensing recognition techniques [53,54].

From the perspective of image analysis techniques, the classification outcomes in this work are predicated on pixel extraction, which indispensably produces the "pretzel phenomenon". The object-oriented classification approach, however, is based on a certain homogeneity within the feature class for object segmentation to obtain the primitives; thus, it is able to fully utilize the rich spectral information, texture information, contextual semantic information, neighborhood information, and spatial information of high-spatial-resolution images and compensate for the drawbacks of the fragmentation of feature categorization that the conventional pixel-based classification method can readily produce [17]. Subsequent research can extract large-area crops by combining object-oriented and GEE [17] algorithms, on the one hand, with image segmentation as the key technology of object-oriented classification. Selecting the appropriate image segmentation algorithms, understanding in detail the impact of segmentation parameters on the segmentation effect, and finding the optimal segmentation scale are important technical issues to be solved.

6. Conclusions

This study proposes an effective approach for tea plantation identification based on multisource remote sensing data. By fully integrating Sentinel-1 radar and Sentinel-2 optical data and utilizing the SVM-RFE algorithm, this study successfully addressed challenges related to complex terrain and cloud cover, significantly improving the accuracy of tea plantation identification to 95.03%. Through the optimization and integration of high-dimensional features, this study provides a universally applicable technical solution for agricultural remote sensing. The main conclusions are as follows:

(1) The feature selection results for tea plantation extraction indicate that spectral features, vegetation indices, and texture features play crucial roles in identifying tea plantations. The combination of these features significantly improves the accuracy of tea plantation spatial distribution extraction, providing essential support for remote sensing monitoring in complex environments and guiding the direction for feature selection in future research.

(2) By recursively eliminating features using the SVM-RFE algorithm, this study identified the optimal feature combination that affects tea plantation recognition and optimized the classification performance of the model. This method reduces the interference of redundant features, ensures the full utilization of key information in high-dimensional data, significantly improves classification accuracy and efficiency, and provides effective support for tea plantation monitoring in complex terrain areas.

(3) Although this method has advantages in identifying tea plantations, it still has certain limitations. The main problem is that for areas where tea plantations are heavily confused with other vegetation (such as gardens and forests), although the introduction of multisource features improves recognition accuracy, some tea plantations still have spectral and texture similarities with forests and farmland, leading to an increase in classification error rates. Therefore, future research can further introduce more distinctive features, especially for the analysis of differences between tea plantations and other evergreen plants, to reduce confusion.

Author Contributions: Conceptualization, P.X. and J.Q.; methodology, Q.Y.; software, P.X.; validation, P.X., Y.L. and J.X.; formal analysis, P.X.; investigation, X.L.; writing—original draft preparation, P.X.; visualization, P.X.; supervision, J.Q. All authors have read and agreed to the published version of the manuscript.

Funding: The Agricultural Science and Technology Innovation Program (ASTIP) (CAAS-CSAL-202402); the National Key Research and Development Program of China (Grant number: 2022YFD1600703).

Data Availability Statement: Dataset available on request from the authors.

Conflicts of Interest: The authors declare no conflicts of interest.

Appendix A

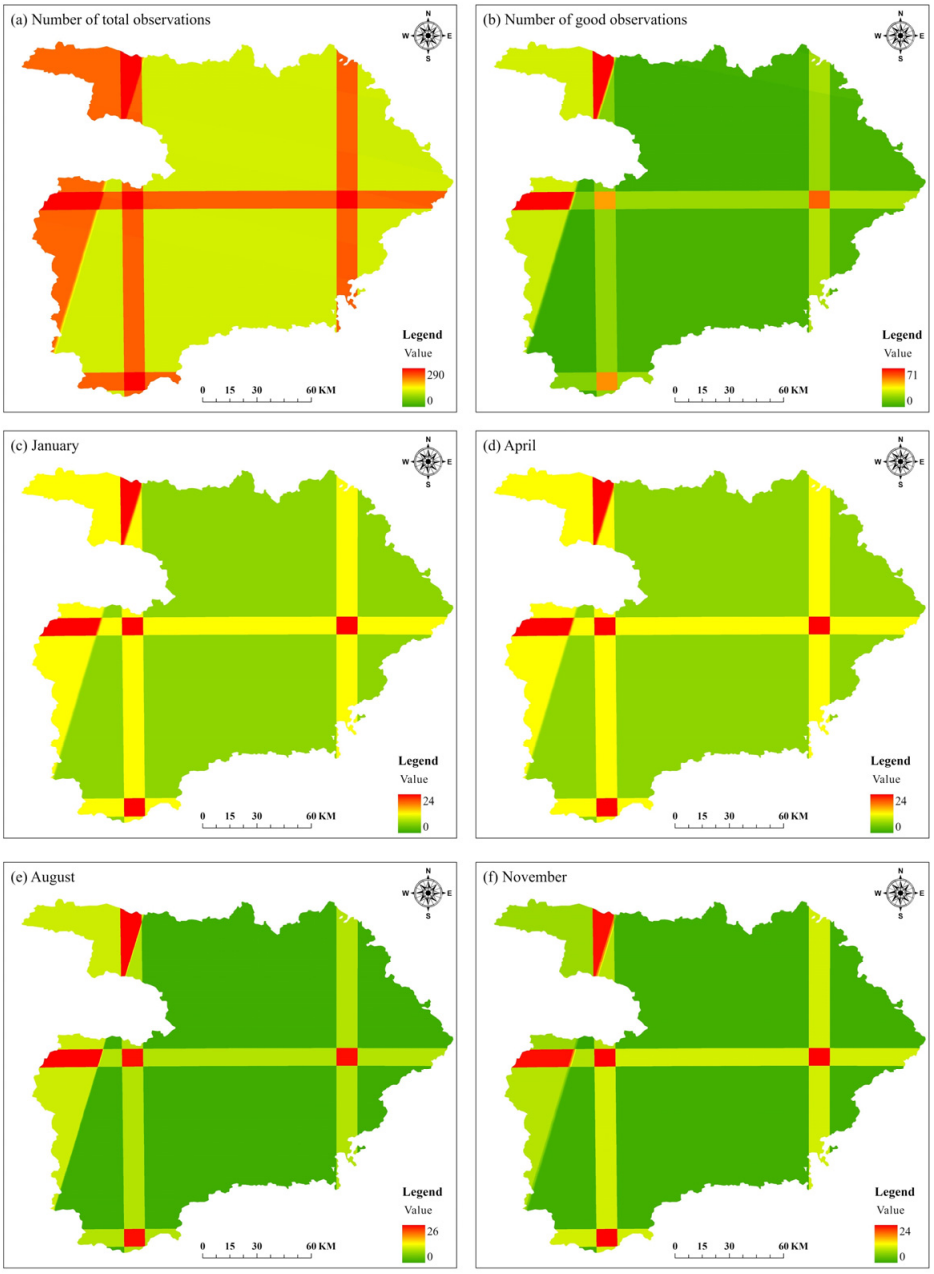


Figure A1. The spatial distribution of the number of (**a**) total observations, (**b**) good observations in 2023, and (**c**–**f**) good observations from Sentinel-2 data in January, April, August, and November.

Appendix B

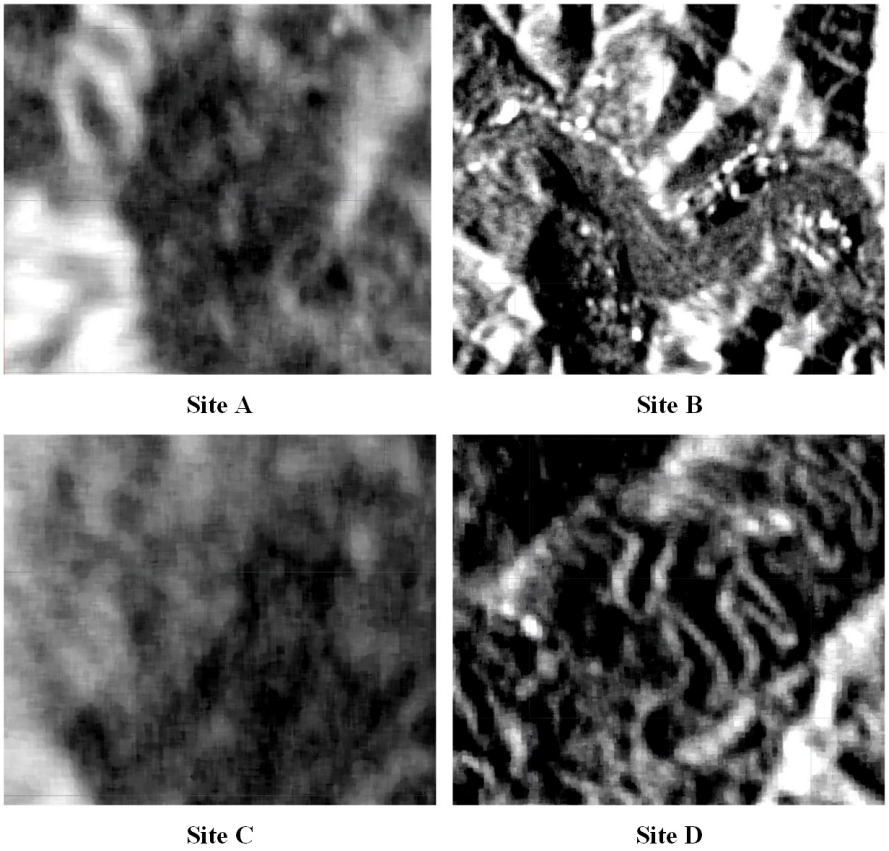


Figure A2. Sentinel-1 SAR image of four selected regions.

References

1. Su, S.; Wan, C.; Li, J.; Jin, X.; Pi, J.; Zhang, Q.; Weng, M. Economic benefit and ecological cost of enlarging tea cultivation in subtropical China: Characterizing the trade-off for policy implications. *Land Use Policy* **2017**, *66*, 183–195. [CrossRef]
2. Bai, J.; Sun, R.; Zhang, H.; Wang, Y.; Jin, Z. Tea plantation identification using GF-1 and Sentinel-2 time series data. *Trans. Chin. Soc. Agric. Eng.* **2021**, *37*, 179–185.
3. Qi, N.; Yang, H.; Shao, G.; Chen, R.; Wu, B.; Xu, B.; Feng, H.; Yang, G.; Zhao, C. Mapping tea plantations using multitemporal spectral features by harmonised Sentinel-2 and Landsat images in Yingde, China. *Comput. Electron. Agric.* **2023**, *212*, 108108. [CrossRef]
4. Xiong, H.; Zhou, X.; Wang, X.; Cui, Y. Mapping the Spatial Distribution of Tea Plantations with 10 m Resolution in Fujian Province Using Google Earth Engine. *J. Geo-Inf. Sci.* **2021**, *23*, 1325–1337.
5. Liang, L.; Wang, J.; Deng, F.; Kong, D. Mapping Pu'er tea plantations from GF-1 images using Object-Oriented Image Analysis (OOIA) and Support Vector Machine (SVM). *PLoS ONE* **2023**, *18*, e0263969. [CrossRef]
6. Xia, H.; Bian, X.; Pan, L.; Li, R. Mapping tea plantation area using phenology algorithm, time-series Sentinel-2 and Landsat images. *Int. J. Remote Sens.* **2023**, *44*, 2826–2846. [CrossRef]
7. Dutta, R.; Smaling, E.M.A.; Bhagat, R.M.; Tolpekin, V.A.; Stein, A. Analysis of factors that determine tea productivity in northeastern India: A combined statistical and modelling approach. *Exp. Agric.* **2012**, *48*, 64–84. [CrossRef]
8. Gilcher, M.; Ruf, T.; Emmerling, C.; Udelhoven, T. Remote Sensing Based Binary Classification of Maize. Dealing with Residual Autocorrelation in Sparse Sample Situations. *Remote Sens.* **2019**, *11*, 2172. [CrossRef]
9. Akar, O.; Guengor, O. Integrating multiple texture methods and NDVI to the Random Forest classification algorithm to detect tea and hazelnut plantation areas in northeast Turkey. *Int. J. Remote Sens.* **2015**, *36*, 442–464. [CrossRef]
10. Haralick, R.M.; Shanmugam, K.; Dinstein, I. Textural Features for Image Classification. *IEEE Trans. Syst. Man Cybern.* **1973**, *SMC-3*, 610–621. [CrossRef]
11. Chuang, Y.C.; Shiu, Y.S. A Comparative Analysis of Machine Learning with WorldView-2 Pan-Sharpened Imagery for Tea Crop Mapping. *Sensors* **2016**, *16*, 594. [CrossRef] [PubMed]

12. Ma, C.; Yang, F.; Wang, X. Extracting tea plantations in southern hilly and mountainous region based on mesoscale spectrum and temporal phenological features. *Remote Sens. Land Resour.* **2019**, *31*, 141–148.
13. Qu, L.A.; Li, M.; Chen, Z.; Liu, W.; Zhi, J.; Zhang, L. Mapping large area tea plantations using progressive random forest and Google Earth Engine. *J. Appl. Remote Sens.* **2022**, *16*, 24509. [CrossRef]
14. Chen, H.; Jiang, H.; Jiang, S. Tea Plantation Extraction Under Object-Oriented Optimal Segmentation Scale. *Geomat. Spat. Inf. Technol.* **2020**, *43*, 17–20.
15. Ramzan, Z.; Asif, H.M.S.; Yousuf, I.; Shahbaz, M. A Multimodal Data Fusion and Deep Neural Networks Based Technique for Tea Yield Estimation in Pakistan Using Satellite Imagery. *IEEE Access* **2023**, *11*, 42578–42594. [CrossRef]
16. Yao, Z.; Zhu, X.; Zeng, Y.; Qiu, X. Extracting Tea Plantations from Multitemporal Sentinel-2 Images Based on Deep Learning Networks. *Agriculture* **2022**, *13*, 10. [CrossRef]
17. Chen, Y.; Tian, S. Comparison of pixel- and object-based image analysis for tea plantation mapping using hyperspectral Gaofen-5 and synthetic aperture radar data. *J. Appl. Remote Sens.* **2020**, *14*, 044516. [CrossRef]
18. Qiu, B.; Yan, C.; Huang, W. Progress and Prospect on Mapping Cropping Systems Using Time Series Images. *J. Geo-Inf. Sci.* **2022**, *24*, 176–188.
19. Chen, P.; Zhao, C.; Duan, D.; Wang, F. Extracting tea plantations in complex landscapes using Sentinel-2 imagery and machine learning algorithms. *Community Ecol.* **2022**, *23*, 163–172. [CrossRef]
20. Gao, S.; Tang, B.; Huang, L.; Chen, G. Identification of tea plantations in typical plateau areas with the combination of Sentinel-1/2 optical and radar remote sensing data based on feature selection algorithm. *Int. J. Remote Sens.* **2024**, *45*, 7033–7053. [CrossRef]
21. Xiao, P.; Qian, P.; Xu, J.; Lu, M. A Bibliometric Analysis of the Application of Remote Sensing in Crop Spatial Patterns: Current Status, Progress and Future Directions. *Sustainability* **2022**, *14*, 4104. [CrossRef]
22. Wang, J.; Xiao, X.; Liu, L.; Wu, X.; Qin, Y.; Steiner, J.L.; Dong, J. Mapping sugarcane plantation dynamics in Guangxi, China, by time series Sentinel-1, Sentinel-2 and Landsat images. *Remote Sens. Environ.* **2020**, *247*, 111951. [CrossRef]
23. Zou, Z.; Xiao, X.; Dong, J.; Qin, Y.; Doughty, R.B.; Menarguez, M.A.; Zhang, G.; Wang, J. Divergent trends of open-surface water body area in the contiguous United States from 1984 to 2016. *Proc. Natl. Acad. Sci. USA* **2018**, *115*, 3810–3815. [CrossRef] [PubMed]
24. Chastain, R.; Housman, I.; Goldstein, J.; Finco, M.; Tenneson, K. Empirical cross sensor comparison of Sentinel-2A and 2B MSI, Landsat-8 OLI, and Landsat-7 ETM+ top of atmosphere spectral characteristics over the conterminous United States. *Remote Sens. Environ.* **2019**, *221*, 274–285. [CrossRef]
25. Huete, A.; Didan, K.; Miura, T.; Rodriguez, E.P.; Gao, X.; Ferreira, L.G. Overview of the radiometric and biophysical performance of the MODIS vegetation indices. *Remote Sens. Environ.* **2002**, *83*, 195–213. [CrossRef]
26. Gao, B. NDWI—A normalized difference water index for remote sensing of vegetation liquid water from space. *Remote Sens. Environ.* **1996**, *58*, 257–266. [CrossRef]
27. Tucker, C.J. Red and photographic infrared linear combinations for monitoring vegetation. *Remote Sens. Environ.* **1979**, *8*, 127–150. [CrossRef]
28. Deventer, V.; Ward, A.D.; Gowda, P.H.; Lyon, J.G. Using Thematic Mapper Data to Identify Contrasting Soil Plains and Tillage Practices. *Photogramm. Eng. Remote Sens.* **1997**, *63*, 87–93.
29. Gitelson, A.A.; Kaufman, Y.J.; Merzlyak, M.N. Use of a green channel in remote sensing of global vegetation from EOS-MODIS. *Remote Sens. Environ.* **1996**, *58*, 289–298. [CrossRef]
30. Huete, A.R. A soil-adjusted vegetation index (SAVI). *Remote Sens. Environ.* **1988**, *25*, 295–309. [CrossRef]
31. Lin, Y.; Zheng, D.; Zhang, Y. Research on the Application of GNDVI Water Body Index Based on GF-6 Images. *Geomat. Spat. Inf. Technol.* **2024**, *47*, 189–191+198.
32. Xu, H. Modification of normalised difference water index (NDWI) to enhance open water features in remotely sensed imagery. *Int. J. Remote Sens.* **2007**, *27*, 3025–3033. [CrossRef]
33. Xiao, X.; Boles, S.; Liu, J.; Zhuang, D.; Frolking, S.; Li, C.; Salas, W.; Moore, B. Mapping paddy rice agriculture in southern China using multi-temporal MODIS images. *Remote Sens. Environ.* **2005**, *95*, 480–492. [CrossRef]
34. Pu, R.; Landry, S. A comparative analysis of high spatial resolution IKONOS and WorldView-2 imagery for mapping urban tree species. *Remote Sens. Environ.* **2012**, *124*, 516–533. [CrossRef]
35. Herold, M.; Woodcock, C.E.; Gregorio, A.D.; Mayaux, P.; Belward, A.S.; Latham, J.; Schmullius, C.C. A joint initiative for harmonization and validation of land cover datasets. *IEEE Trans. Geosci. Remote Sens.* **2006**, *44*, 1719–1727. [CrossRef]
36. Gu, M.; Su, B.; Wang, M.; Wang, Z. Survey on decolorization methods. *Appl. Res. Comput.* **2019**, *36*, 1286–1292.
37. Fan, D.; Zhao, X.; Zhu, W.; Zheng, Z. Review of influencing factors of accuracy of plant phenology monitoring based on remote sensing data. *Prog. Geogr.* **2016**, *35*, 304–319.
38. Liu, S.; Liu, M.; Li, G.; Wang, M.; Ma, C.; Fu, Y.; Hou, F.; Liu, Y. A review of research progress in plant phenology. *Pratacult. Sci.* **2024**, *41*, 2402–2418.
39. Li, N.; Zhang, D.; Li, L.; Zhang, Y. Mapping the Spatial Distribution of Tea Plantations Using High-Spatiotemporal-Resolution Imagery in Northern Zhejiang, China. *Forests* **2019**, *10*, 856. [CrossRef]

40. Descals, A.; Verger, A.; Yin, G.; Peñuelas, J. Improved Estimates of Arctic Land Surface Phenology Using Sentinel-2 Time Series. *Remote Sens.* **2020**, *12*, 3738. [CrossRef]
41. Guo, Y.; Ren, H. Remote sensing monitoring of maize and paddy rice planting area using GF-6 WFV red edge features. *Comput. Electron. Agric.* **2023**, *207*, 107714. [CrossRef]
42. Zoungrana, L.E.; Barbouchi, M.; Toukabri, W.; Babasy, M.O.; Khatra, N.B.; Annabi, M.; Bahri, H. Sentinel SAR-optical fusion for improving in-season wheat crop mapping at a large scale using machine learning and the Google Earth engine platform. *Appl. Geomat.* **2024**, *16*, 147–160. [CrossRef]
43. Schulthess, U.; Rodrigues, F.; Taymans, M.; Bellemans, N.; Bontemps, S.; Ortiz-Monasterio, I.; Gérard, B.; Defourny, P. Optimal Sample Size and Composition for Crop Classification with Sen2-Agri's Random Forest Classifier. *Remote Sens.* **2023**, *15*, 608. [CrossRef]
44. Monsalve-Tellez, J.M.; Torres-León, J.L.; Garcés-Gómez, Y.A. Evaluation of SAR and Optical Image Fusion Methods in Oil Palm Crop Cover Classification Using the Random Forest Algorithm. *Agriculture* **2022**, *12*, 955. [CrossRef]
45. Mandal, D.; Kumar, V.; Rao, Y.S. An assessment of temporal RADARSAT-2 SAR data for crop classification using KPCA based support vector machine. *Geocarto Int.* **2022**, *37*, 1547–1559. [CrossRef]
46. Saini, R.; Ghosh, S.K. Crop Classification on Single Date SENTINEL-2 Imagery Using Random Forest and Support Vector Machine. *Int. Arch. Photogramm. Remote Sens. Spat. Inf. Sci.* **2018**, *XLII-5*, 683–688. [CrossRef]
47. Peng, Y.; Qiu, B.; Tang, Z.; Xu, W.; Yang, P.; Wu, W.; Chen, X.; Zhu, X.; Zhu, P.; Zhang, X.; et al. Where is tea grown in the world: A robust mapping framework for agroforestry crop with knowledge graph and sentinels images. *Remote Sens. Environ.* **2024**, *303*, 114016. [CrossRef]
48. Huang, S.; Xu, W.; Wu, C.; Dai, Y.; Kou, W. Research Progress of Remote Sensing on Tea Plantation Monitoring. *J. West China For. Sci.* **2020**, *49*, 1–9.
49. Phan, P.; Chen, N.; Xu, L.; Chen, Z. Using Multi-Temporal MODIS NDVI Data to Monitor Tea Status and Forecast Yield: A Case Study at Tanuyen, Laichau, Vietnam. *Remote Sens.* **2020**, *12*, 1814. [CrossRef]
50. Parida, B.R.; Mahato, T.; Ghosh, S. Monitoring tea plantations during 1990–2022 using multi-temporal satellite data in Assam (India). *Trop. Ecol.* **2024**, *65*, 387–398. [CrossRef]
51. Huang, X.; Zhu, Z.; Li, Y.; Wu, B.; Yang, M. Tea Garden Detection from High-Resolution Imagery Using a Scene-Based Framework. *Photogramm. Eng. Remote Sens.* **2018**, *84*, 723–731. [CrossRef]
52. Chen, Y.; Lin, J.; Yang, Y.; Wang, X. Extraction of tea plantation with high resolution Gaofen-2 image. In Proceedings of the 2019 8th International Conference on Agro-Geoinformatics (Agro-Geoinformatics), Istanbul, Turkey, 16–19 July 2019; pp. 1–6.
53. Zhang, Q.; Wan, B.; Cao, Z.; Zhang, Q.; Wang, D. Exploring the Potential of Unmanned Aerial Vehicle (UAV) Remote Sensing for Mapping Plucking Area of Tea Plantations. *Forests* **2021**, *12*, 1214. [CrossRef]
54. Yuan, L.; Yu, Q.; Zhang, Y.; Wang, X.; Xu, O.; Li, W. Monitoring Thosea sinensis Walker in Tea Plantations Based on UAV Multi-Spectral Image. *Phyton-Ann. REI Bot.* **2023**, *92*, 747–761. [CrossRef]

Disclaimer/Publisher's Note: The statements, opinions and data contained in all publications are solely those of the individual author(s) and contributor(s) and not of MDPI and/or the editor(s). MDPI and/or the editor(s) disclaim responsibility for any injury to people or property resulting from any ideas, methods, instructions or products referred to in the content.